Unified Approach to Cycloid Drive Profile, Stress, and Efficiency Optimization

Jonathon W. Sensinger
Department of Physical Medicine and Rehabilitation,
Northwestern University,
345 E. Superior Street,
Chicago, IL 60611;
Neural Engineering Center for Artificial Limbs,
Rehabilitation Institute of Chicago,
345 E. Superior Street,
Chicago, IL 60611
e-mail: sensinger@ieee.org

Cycloid drives are compact, efficient speed reducers. In this paper, a unified set of equations is presented to optimize their design. The conceptual framework and profile design are described. Sources and effects of tolerance are then introduced, including profile reduction, backlash and torque ripple, and maximum gear-ratio. Equations for stress, efficiency, and moment of inertia are provided. [DOI: 10.1115/1.4000832]

1 Introduction

Cycloid drives are compact, high-ratio speed reducers commonly used in boats and large equipment due to their ability to withstand large loads. Their compact size and high efficiency make them suitable for smaller-scale robotics as well, although they have received relatively little attention in the field of robotics compared with a similar gear: the harmonic drive [1–3]. Harmonic and cycloid drives are appropriate for different subsets of robotics: harmonic drives excel in those applications requiring no backlash and precise output positions, whereas cycloid drives excel in applications requiring large torque, maximum efficiency, and low noise.

Numerous authors have advanced several aspects of the design theory of cycloid drives, including profile generation [4,5], avoidance of undercutting and discontinuities [6–8], and calculation of backlash and gear-ratio ripple. Due to the unique geometry of cycloid drives, they have used different frameworks to assess the parameter of interest. In the resulting literature, therefore, different reference frames and variables were used, making it difficult to optimize a cycloid drive with respect to all of the parameters. In addition, there are several gaps in literature pertaining to cycloid drive optimization, such as a thorough treatment of tolerance, calculation of gear-ratio and maximum allowable gear-ratio in the presence of tolerances, stress calculations, efficiency estimation and optimization, optimization of output-hole placement, and calculation of the reflected moment of inertia (MOI).

The purpose of this paper is to present a unified treatment of cycloid drives that may be used by designers of both large equipment and smaller robots and to provide all of the necessary closed-form equations to optimize any cycloid drive and compare it with other gear transmissions.

Contributed by the Power Transmission and Gearing Committee of ASME for publication in the JOURNAL OF MECHANICAL DESIGN. Manuscript received March 9, 2009; final manuscript received December 4, 2009; published online February 9, 2010. Assoc. Editor: Philippe Velex.

2 Unified Design Approach

2.1 Conceptual Framework. Cycloid drives contain three main elements: an input shaft, an output disk, and an intermediate cycloid disk that wobbles relative to the output disk when spun by the input shaft (Fig. 1). The input shaft includes an eccentric cam, which drives the cycloid disk in an eccentric, cycloidal motion with respect to stationary rollers on the perimeter. The cycloid disk also rotates with respect to the input shaft. The radial motion of the disk is not translated to the output shaft. There is typically a ball bearing between the input cam and the cycloid disk, bushings between the rollers and the casing, and bushings between the output holes of the cycloid disk and the output pins of the output disk.

The cycloid disk in a cycloid drive has Z_1 number of lobes. For the epitrochoid designs considered in this paper, there are Z_2 rollers, where Z_2 is an integer higher than Z_1. The rollers have radius R_r and are located a distance R away from the center and the cycloid disk spins about this center on an eccentric cam with radius e (Fig. 2). From these parameters the gear-ratio (GR) is

$$\mathrm{GR} = \frac{\omega_{\mathrm{input}}}{\omega_{\mathrm{output}}} = \frac{Z_1}{Z_2 - Z_1} \tag{1}$$

where ω_{input} is the angular velocity of the input shaft and ω_{output} is the angular velocity of the output disk. From this equation, it may be seen that the gear-ratio is maximum when $Z_2 - Z_1$ equals 1. Thus, it seems disadvantageous to design a tooth difference greater than 1. This conclusion is strengthened by the observation that for a tooth difference Δ equal to 1, all of the lobes may be engaged, resulting in extremely low stress; whereas for Δ greater than 1, fewer than half of the lobes will be in contact even with an optimized design that does not consider tolerances [9]. Accordingly, the remainder of this paper will present equations only for the constrained class of Δ equal to 1.

2.2 Profile. The cycloid profile C (Fig. 2(*c*)) may be mathematically generated using equations derived by Shin and Kwon [4]:

$$\begin{aligned} C_x &= R\cos\phi - R_r\cos(\phi+\psi) - e\cos((Z_1+1)\phi) \\ C_y &= -R\sin\phi + R_r\sin(\phi+\psi) + e\sin((Z_1+1)\phi) \end{aligned} \tag{2}$$

where ϕ is the angle of the input shaft and ψ is the contact angle between the cycloid lobe and roller calculated as

$$\psi = \tan^{-1}\left[\frac{\sin(Z_1\phi)}{\cos(Z_1\phi) - \dfrac{R}{e(Z_1+1)}}\right] \tag{3}$$

It is important when designing a cycloid drive to ensure that undercutting does not occur and that the rollers do not intersect each other. The existence of undercutting may be found by any of the three manipulations of the equation derived by Ye et al. [8]:

$$R_{r\,\max} = \sqrt{\frac{27Z_1[R^2 - e^2(Z_1+1)^2]}{(Z_1+2)^3}}$$

$$R_{\min} = \sqrt{\frac{R_r^2(Z_1+2)^3}{27Z_1} + e^2(Z_1+1)^2}$$

and

$$e_{\max} = \sqrt{\frac{27R^2Z_1 - R_r^2(Z_1+2)^3}{27Z_1(Z_1+1)^2}} \tag{4}$$

The rollers must be small enough that they do not intersect each other [4,6]. This constraint may be found by

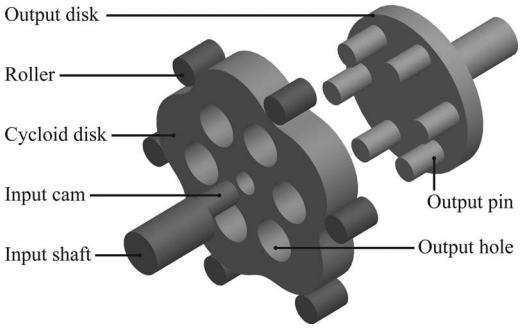

Fig. 1 Main components in a cycloid drive

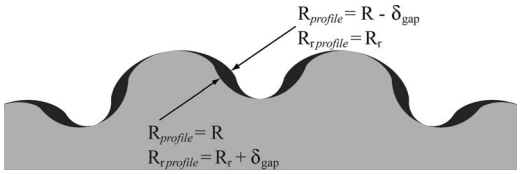

Fig. 3 Cycloid disk profile may be reduced to account for tolerance by increasing R_r or reducing R: these adjustments result in a different inflection between the peaks

$$R_{r\,\max} = R \sin\left(\frac{\pi}{Z_1 + 1}\right) \tag{5}$$

Equations (4) and (5) should be evaluated using values of R and R_r that incorporate the profile reductions necessary to accommodate tolerances, as explained in the next section.

2.3 Tolerance and Machining. The cycloid profile must be reduced to account for tolerance in machining, which will affect the backlash, torque ripple, and maximum obtainable gear-ratio.

2.3.1 Cycloid Profile Reduction. Offset tolerances include tolerances of the input cam eccentricity δ_{eo}, the offset of the holes in the ground structure for the rollers δ_R, the offset of the input shaft of the cycloid disk δ_{CS}, and the profile of the cycloid drive δ_{CP}. The axial-play tolerances may be omitted from the profile reduction calculations because they cannot cause unintended collisions.

Tolerance δ_R should be incorporated by reducing R. Tolerance δ_{eo} and δ_{CS} are best modeled by reducing R as well since they are offset variables rather than curvature variables. Tolerance δ_{CP} may be incorporated into either R or R_r. The simplest equation occurs when δ_{CP} is incorporated into R as well.

An absolute tolerance system [10] should be used when designing the cycloid profile. Assuming the radial tolerance of the rollers is negligible, the cycloid profile may be generated by reducing R for the generation of the cycloid disk profile to obtain $R_{profile}$ as follows:

$$\delta_{gap} = \delta_{eo} + \delta_R + \delta_{CS} + \delta_{CP} \tag{6}$$

$$R_{profile} = R - \delta_{gap} \tag{7}$$

This recommendation is in contrast to Yang and Blanche [11], who only consider the tolerance of the cycloid disk, and who recommend that R_r should be modified to account for the cycloid tolerance. Modifying R instead of R_r changes the profile in between the peaks and valleys. The contrast between these two compensations (Fig. 3) is most pronounced when the profile is close to the undercutting boundary. The undercutting constraint must be re-evaluated using $R_{profile}$ instead of R.

2.3.2 Torque Ripple and Backlash. The axial-play in the journal bearings of the rollers δ_{JB} is typically equal to $0.001R_r$ [12] and must be included in backlash, torque ripple, and maximum gear calculations, which are all limited by a loss of contact between components. The value of δ_{JB} should be incorporated into R. The intentional reduction in the cycloid profile δ_{gap} must also be included. For calculation of backlash and torque ripple, a statistical tolerance system is more accurate—although less conservative—than the absolute tolerance system [10] for which

$$\delta_{sum} = \sqrt{\delta_{eo}^2 + \delta_R^2 + \delta_{CS}^2 + \delta_{CP}^2 + \delta_{JB}^2} + \delta_{gap} \tag{8}$$

Yang and Blanche [11] calculated the effect of the tolerance of the cycloid profile on backlash and gear-ratio fluctuation. These results may be extended by incorporating the other sources of tolerance and simplified by algebraic manipulation. The maximum amount of backlash for a given design is accordingly estimated by

$$\mathrm{BL} = \pm \frac{\delta_{sum}}{eZ_1}\mathrm{rad} \tag{9}$$

The maximum percentage of gear-ratio fluctuation for a given design is estimated by

$$\mathrm{GR}_f = 5.35\frac{\delta_{sum} Z_1}{e(Z_1 + 1)} \tag{10}$$

2.3.3 Maximum Gear-Ratio. The maximum gear-ratio is limited by either the outer diameter of the transmission and the tolerance of the system or the intersection of the rollers. The tolerance calculations for the maximum gear-ratio must include axial-

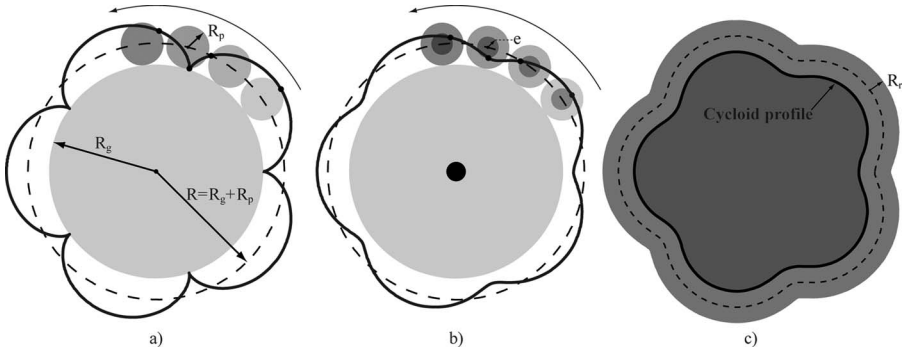

Fig. 2 Conceptualization of cycloid disk profile: (*a*) the profile may be visualized by tracing a point on a generating circle as it rolls around a base circle, (*b*) a point inside of the generating circle is used to avoid undercutting, and (*c*) the roller radius is subtracted from the resulting trajectory to create the disk profile (outline of dark gray area)

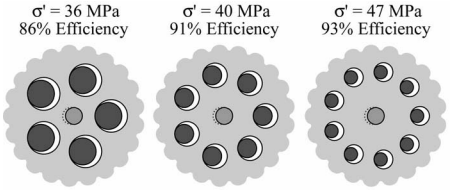

Fig. 4 Efficiency and stress increase as output-hole radius decreases and distance from center increases

play but should use the more conservative absolute tolerance system instead of the statistical tolerance system to present a worst-case scenario. Thus,

$$\delta_{GR} = 2\delta_{gap} + \delta_{JB} \tag{11}$$

Cam eccentricity must be larger than half of δ_{GR} to ensure that the rollers contact the cycloid drive. By reworking the undercutting constraint using $\frac{1}{2}\delta_{GR}$ in place of e, the maximum GR may be defined as

$$(R_r^2 + 6.75\delta_{GR}^2)GR_{max}^3 + (6R_r^2 + 13.5\delta_{GR}^2 - 27R^2)GR_{max}^2 + 6.75\delta_{GR}^2 GR + 8R_r^2 = 0 \tag{12}$$

This cubic equation may be solved using Cardano's method and is conservatively estimated by

$$GR_{max} = \frac{3R}{2\delta_{GR}} - 1 \tag{13}$$

using discontinuity constraints. The roller intersection constraint, which may also limit the maximum gear-ratio for small-diameter rollers, may be found by reworking Eq. (5).

3 Remaining Design Constraints

Once the cycloid disk profile has been designed, the cycloid depth and the location of the output holes must be defined. In addition to the intended rotational movement produced in a cycloid, there is also a translational movement due to the eccentric cam. In order to transmit only the rotational motion, the output holes in the cycloid disk have a larger diameter than the output pins inset into the output shaft. As the cycloid rotates, the output pins are pushed against the output holes in the cycloid disk, resulting in rotational movement of the output shaft (Fig. 4). The radius of the output holes should be equal to the radius of the output pins plus the offset of the cam e in addition to the tolerance of machining.

3.1 Stress. In contrast to harmonic drives and many other gear systems, the stresses encountered in a cycloid disk are solely compressive. There is no shear stress between the cycloid lobes and rollers, although double shear may exist at the interface of the rollers and the bushings for some designs. This property allows a given cycloid drive with the same material properties and dimensions as other gears to withstand substantially higher loads since conventional materials can withstand double the amount of compressive stress as compared with shear stress [10].

The stress transmitted from the cycloid disk to the rollers and from the output holes to the output pins may be modeled using Hertz's model of cylindrical contact [10]. The von Mises stress may be calculated as

$$\sigma' = \frac{2F}{\pi bt}(3 + 4\upsilon^2) \tag{14}$$

where F is the applied force, t is the thickness of the contact, and b is the width of the contact caused by the deformed materials defined as

$$b = \sqrt{\frac{4F}{\pi l}\frac{(1-\upsilon_1^2)/E_1 + (1-\upsilon_2^2)/E_2}{1/R_1 + 1/R_2}} \tag{15}$$

For the case of the cycloid disk in contact with the rollers, $R_1 = R_r$ and

$$R_2 = \frac{(R - eZ_1 - e)^3}{R - e(Z_1 - 1)^2} - R_r \tag{16}$$

where R_1 is positive and R_2 is negative. Equation (16) may found by simplifying Eq. (8) in the paper of Ye et al. [8] for the case when ϕ_2 equals 0. The compressive force at the interface between the cycloid disk and the rollers is

$$F = \frac{T}{R - R_r} \tag{17}$$

where T is the applied output torque. For a tooth difference (Δ) of 1 and perfect construction, all of the cycloid disk lobes are in contact at all times. Once tolerance is introduced, however, only one of the lobes engages at a time, although the other lobes may engage once the disk deforms if the tolerances are small.

When calculating the stress between the output pins and output holes, the radius of the output holes in Eq. (15) is negative. Stress is inversely proportional to the number of holes and the radius of these holes (Fig. 4).

In addition to the compressive stress encountered between the cycloid disk and the rollers, the rollers may encounter shear stress at the junction with the bushings for some designs. Since the rollers are typically made from hardened steel, these stresses are usually relatively negligible but as the roller radius shrinks, the shear stress becomes more relevant.

Finally, a radial force will be exerted on the bearing attached to the eccentric cam

$$F_{cam} = \frac{T}{eZ_1} \tag{18}$$

Depending on the value of e and gear-ratio Z_1, this radial force may be high and care should be taken in choosing the bearing to ensure the cycloid drive does not fail at this point [13].

3.2 Efficiency. The efficiency of cycloid drives is influenced by frictional loses at the input bearing, the interface between the cycloid disk and the rollers, and the interface between the output holes of the cycloid disk and the pins of the output disk. The input bearings are typically ball bearings, which usually have efficiencies of 99.8%. Frictional losses between the cycloid drive and roller interface occur within the journal bearing of the roller. The output pins are also journal bearings for which efficiency is

$$\eta = 1 - \mu\frac{R_e}{\rho_e} \tag{19}$$

where R_e is the radius of pin or cycloid tooth and ρ_e is the offset of the pin or cycloid tooth from the center of the cycloid [10]. The efficiency of the output pins will always be worse than the efficiency of the cycloid lobes because r is often larger and ρ_e is always smaller. The efficiency of the cycloid drive improves as the output pins become smaller and move farther away from the center (Fig. 4).

Cycloid drive efficiency is independent of gear-ratio and applied load since frictional loses at the journal bearings scale with the applied load. Thus, unlike planetary gears and harmonic drives, which only have maximum efficiency at full loads, cycloid drives maintain high efficiency throughout the load range. This efficiency is illustrated in Fig. 5, which compares normalized, comparable efficiency ratings modeled from a MicroMo Electronics (Clearwater, FL) 134:1 planetary gear, a Harmonic Drive LLC (Hauppauge, NY) HD-CSD-20 100:1 drive, and the cycloid

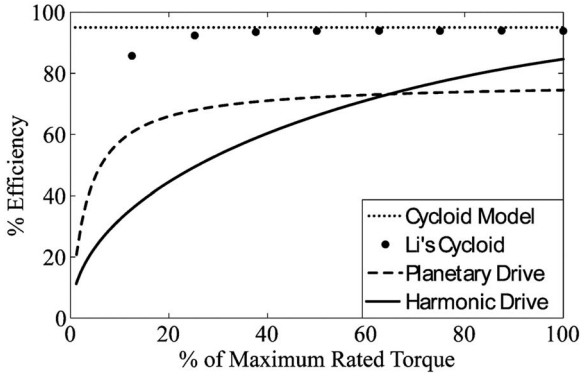

Fig. 5 Cycloid drives have high efficiency independent of torque: the calculated efficiency of cycloid drives can be significantly higher than harmonic drives and planetary gears

model. The measured cycloid efficiency published by Li et al. [13] was also shown to validate the predicted high efficiency of the cycloid drive.

3.3 Reflected Moment of Inertia. The moment of inertia is an important parameter in the optimization of robotic transmissions, especially for the case of large gear-ratios. This calculation must accommodate the off-axis center-of-mass rotation of several of the components. The moment of inertia calculations may be categorized by their rotational speeds as follows:

- Objects rotating at input speed
  - eccentric cam rotation
  - center-of-mass off-axis rotation (parallel axis theorem)
    - cycloid disk
    - eccentric cam
    - ball bearing
- Objects rotating at output speed
  - cycloid disk rotation
  - output disk rotation
- Rollers in contact with the cycloid disk

3.3.1 Objects Rotating at Input Speed. The eccentric cam rotates at the input speed. Its moment of inertia may be calculated using the formula for a cylinder. The cycloid disk, eccentric cam, and ball bearing are all offset from the input axis. As a result, the effect of their offset on the moment of inertia must be calculated using the parallel axis theorem $J' = me^2$, where m is the mass of the object. The area of the cycloid disk profile is well approximated by

$$\text{Area}_{\text{CD profile}} \approx \pi(R - R_r)^2 \tag{20}$$

from which the mass may be calculated. This approximation has greater than 95% accuracy compared with the area calculated using finite element analysis (FEA) software.

These moments of inertia are multiplied by the square of the gear-ratio to calculate the reflected inertia at the output shaft:

$$J^*_{\text{input}} = Z_1^2[J_{\text{cam}} + e^2(m_{\text{cam}} + m_{\text{ball bearing}} + m_{\text{cycloid disk}})] \tag{21}$$

3.3.2 Objects Rotating at Output Speed. The closed-form calculation of the inertia of the cycloid disk is difficult due to the inclusion of the tangent expression in the ψ term of Eq. (3). However, the equation may be simplified by ignoring the R_r term. R may be reduced by R_r to accommodate this omission. When these simplifications are made, the inertia of the cycloid disk may be calculated as

$$J_{\text{CD profile}} \approx \frac{t\rho\pi}{2}((R - R_r)^4 + e^4 + 4e^2(R - R_r)^2) \tag{22}$$

This simplified equation has greater than 95% accuracy compared with the value calculated using FEA software. Once the moment of inertia of the cycloid disk has been calculated, the moment of inertia of the cam hole and the output holes must be subtracted to obtain J_{CD}. The moment of inertia of the output disk and pins (J_{OD}) may be calculated using the formula for a cylinder.

3.3.3 Moment of Inertia of the Rollers. Any rollers that are in contact with the cycloid disk will also contribute a reflected moment of inertia. For the case in which tolerance has been accommodated, only one roller will engage at a time. The speed of the roller relative to the output speed is equal to $(R/R_r) - 1$ in which case the reflected moment of inertia of the roller is

$$J^*_{\text{roller}} = \left(\frac{R}{R_r} - 1\right)^2 J_{\text{roller}} \tag{23}$$

3.3.4 Total Reflected Inertia. The total reflected output inertia as seen by the output may then be found by summing Eqs. (21)–(23), as well as J_{OD}, to obtain

$$J^*_{\text{cycloid drive}} = Z_1^2[J_{\text{cam}} + e^2(m_{\text{cam}} + m_{\text{ball bearing}} + m_{\text{CD}})] + \left(\frac{R}{R_r} - 1\right)^2 J_{\text{roller}} + J_{\text{CD}} + J_{\text{OD}} \tag{24}$$

4 Discussion

Cycloid drives use a unique profile to achieve a high gear-ratio in a compact package. The compressive nature of the stresses involved in the transmission allows them to withstand high loads compared with similar gears. The fact that roller bearings are used to transmit the torque allows the drive to have extremely high efficiencies, even for large gear-ratios or low torques. Cycloid drives are therefore a valuable transmission both for large-scale equipment and for robotic applications in which efficiency and strength are required in a compact package.

Cycloid drives must usually be custom machined due to their profile. Such processes typically result in larger tolerances than found in standardized teeth profiles machined in planetary gears. As a result, the backlash and gear-ratio ripple in cycloid drives must be calculated when considering their use in any application and the maximum gear-ratio will be limited by the tolerances of the parts and the strength of the materials.

Nomenclature

$\text{Area}_{\text{CD profile}}$ = area of cycloid disk
E = modulus of elasticity
F = force
GR_{max} = maximum gear-ratio
GR_f = gear-ratio fluctuation
$J^*_{\text{cycloid drive}}$ = reflected MOI of cycloid drive
J^*_{input} = reflected MOI of components moving at input speed
J^*_{roller} = reflected MOI of roller
J_{cam} = MOI of eccentric cam
J_{CD} = MOI of cycloid disk
J_{OD} = MOI of output disk
$J_{\text{output components}}$ = MOI of components moving at output speed
J_{roller} = MOI of roller
R = offset of rollers
$R1, R2$ = radii of cylinders
R_e = radius used to calculate efficiency
R_G = radius of generating circle
R_p = radius of base circle

$R_{profile}$ = offset of rollers used when calculating reduced profile
R_r = radius of rollers
T = torque
Z_1 = number of cycloid lobes
Z_2 = number of rollers
b = width of deformed contact
e = eccentricity of cam
m = mass
t = thickness
Δ = difference between the number of lobes and rollers
δ_{CP} = tolerance of cycloid drive profile
δ_{CS} = tolerance of cycloid drive input hole offset
δ_{eo} = tolerance of cam eccentricity
δ_{gap} = tolerance used to reduce cycloid profile
δ_{GR} = tolerance used to calculate maximum gear-ratio
δ_{JB} = axial-play in roller bearing
δ_R = tolerance of roller offset
δ_{sum} = tolerance used to calculate backlash and torque ripple
ϕ = input angle
η = efficiency
μ = coefficient of friction
ρ = density
ρ_e = offset of pin
σ' = von Mises stress
υ = Poisson's ratio
ψ = contact angle

References

[1] Hashimoto, M., Kiyosawa, Y., and Paul, R. P., 1993, "A Torque Sensing Technique for Robots With Harmonic Drives," IEEE Trans. Rob. Autom., **9**, pp. 108–116.
[2] Kennedy, C. W., and Desai, J. P., 2003, "Estimation and Modeling of the Harmonic Drive Transmission in the Mitsubishi PA-10 Robot Arm," IEEE International Conference on Intelligent Robotics and Systems, Las Vegas, NV.
[3] Albu-Schaffer, A., Eiberger, O., Grebenstein, M., Haddadin, S., Ott, C., Wimbock, T., Wolf, S., and Hirzinger, G., 2008, "Soft Robotics—From Torque Feedback-Controlled Lightweight Robots to Intrinsically Compliant Systems," IEEE Rob. Autom. Mag., **15**, pp. 20–30.
[4] Shin, J. H., and Kwon, S. M., 2006, "On the Lobe Profile Design in a Cycloid Reducer Using Instant Velocity Center," Mech. Mach. Theory, **41**, pp. 596–616.
[5] Gorla, C., Davoli, P., Rosa, F., Longoni, C., Chiozzi, F., and Samarani, A., 2008, "Theoretical and Experimental Analysis of a Cycloidal Speed Reducer," ASME J. Mech. Des., **130**, p. 112604.
[6] Hwang, Y. W., and Hsieh, C. F., 2007, "Geometric Design Using Hypotrochoid and Nonundercutting Conditions for an Internal Cycloidal Gear," ASME J. Mech. Des., **129**, pp. 413–420.
[7] Mimmi, G. C., and Pennacchi, P. E., 2000, "Non-Undercutting Conditions in Internal Gears," Mech. Mach. Theory, **35**, pp. 477–490.
[8] Ye, Z. H., Zhang, W., Huang, Q. H., and Chen, C. M., 2006, "Simple Explicit Formulae for Calculating Limit Dimensions to Avoid Undercutting in the Rotor of a Cycloid Rotor Pump," Mech. Mach. Theory, **41**, pp. 405–414.
[9] Chen, B., Fang, T. T., Li, C. Y., and Wang, S. Y., 2008, "Gear Geometry of Cycloid Drives," Sci. China, Ser. E: Technol. Sci., **51**, pp. 598–610.
[10] Shigley, J. E., Mischke, C. R., and Budynas, R. G., 2004, *Mechanical Engineering Design*, 7th ed., McGraw-Hill, New York.
[11] Yang, D. C. H., and Blanch, J. G., 1990, "Design and Application Guidelines for Cycloid Drives With Machining Tolerances," Mech. Mach. Theory, **25**, pp. 487–501.
[12] Harnoy, A., 2002, *Bearing Design in Machinery: Engineering Tribology and Lubrication*, CRC, New York, NY.
[13] Li, X., He, W. D., Li, L. X., and Schmidt, L. C., 2004, "A New Cycloid Drive With High-Load Capacity and High Efficiency," ASME J. Mech. Des., **126**, pp. 683–686.